

Rhodium–Hydrogen–Tin Three-Center Bonds. NMR (^1H , ^{31}P , ^{103}Rh , ^{119}Sn) Study of $[\text{Rh}(\text{Cl})(\text{H})(\text{SnPh}_3)(\text{PPh}_3)(\text{py})]$ and Related Compounds

Laurence Carlton

Centre for Molecular Design, Department of Chemistry, University of the Witwatersrand, Johannesburg, Republic of South Africa

Received August 31, 1999

The complex *trans*- $[\text{Rh}(\text{NCBPh}_3)(\text{H})(\text{SnPh}_3)(\text{PPh}_3)_2]$ (**1**) reacts with pyridine and substituted pyridines (L) in dichloromethane at 22 °C to give $[\text{Rh}(\text{NCBPh}_3)(\text{H})(\text{SnPh}_3)(\text{PPh}_3)(\text{L})]$ (**2a**) and at –25 °C to give *trans*- $[\text{Rh}(\text{NCBPh}_3)(\text{H})(\text{SnPh}_3)(\text{PPh}_3)_2(\text{L})]$ (**3a**). These complexes and numerous analogues can be prepared (the majority in solution only) by the reactions of $[\text{Rh}(\text{X})(\text{PPh}_3)_3]$ (X = NCBPh₃ (**a**), N(CN)₂ (**b**), NCS (**c**), N₃ (**d**), NCO (**e**), O₂CCF₃ (**f**), Cl (**g**)) with Ph₃SnH in solutions containing pyridines (4-Rpy; R = CO₂Me, H, NMe₂), 1-methylimidazole (1-Meim), and benzonitriles (4-RC₆H₄CN; R = COMe, H, NMe₂) (L). NMR data for the series of complexes **2** in which ligands X, L, and, for X = Cl, the phosphine P(4-C₆H₄R)₃ (R = F, H, Me) were varied independently show systematic changes in the parameters $\delta(^{119}\text{Sn})$, $\delta(^{103}\text{Rh})$, $J(^{119}\text{Sn}-^1\text{H})$, and $J(^{103}\text{Rh}-^{119}\text{Sn})$, which are related to the electron-donating properties of X, L, and the phosphine. Plots of $J(^{119}\text{Sn}-^1\text{H})$ against $\delta(^{119}\text{Sn})$, $\delta(^{103}\text{Rh})$, and $J(^{103}\text{Rh}-^{119}\text{Sn})$ are approximately linear and show $\delta(^{103}\text{Rh})$ and $J(^{103}\text{Rh}-^{119}\text{Sn})$ increasing with $J(^{119}\text{Sn}-^1\text{H})$ and $\delta(^{119}\text{Sn})$ decreasing. Complexes **3** give higher values of $J(^{119}\text{Sn}-^1\text{H})$ and lower values of $\delta(^{119}\text{Sn})$ than found for the less electron-rich **2**, with data for **3** continuing the trends in $J(^{119}\text{Sn}-^1\text{H})$ and $\delta(^{119}\text{Sn})$ observed for **2**. Values of $\delta(^{103}\text{Rh})$ and $J(^{103}\text{Rh}-^{119}\text{Sn})$ for **3** do not match the pattern found for **2**; nor do data for an isomeric form of **3**, *cis*- $[\text{Rh}(\text{Cl})(\text{H})(\text{SnPh}_3)(\text{PR}_3)_2(\text{L})]$ (L = benzonitriles) (**4**). The plot of $J(^{119}\text{Sn}-^1\text{H})/\delta(^{119}\text{Sn})$ for **3** shows discontinuities at high values of $J(^{119}\text{Sn}-^1\text{H})$, with the trend in $\delta(^{119}\text{Sn})$ toward more negative values (as the ligands become more nucleophilic) being transformed into an increase and changes in $J(^{119}\text{Sn}-^1\text{H})$ becoming smaller. These patterns of NMR data are interpreted in terms of the weakening of an Rh–(H–Sn) three-center interaction and changes in the coordination geometry of tin as the electron density on rhodium is increased.

Introduction

Three-center bonded “agostic”¹ interactions, involving a transition metal, hydrogen, and carbon, have been the focus of much research into the activation of C–H bonds and the search for catalytic systems that can usefully derivatize alkanes.² Although the characterization of such bonds has relied heavily on diffraction studies,^{3,4} a very useful role for NMR spectroscopy in the identification of three-center bonds was recognized some years ago by Green and co-workers.^{1,3} On complexation of a C–H bond to a transition metal to form an agostic bond,

a change occurs in the magnitude of the carbon–hydrogen spin-coupling constant, which falls to a value significantly lower than that of the uncomplexed hydrocarbon but substantially higher than that of the full oxidative addition product in which the C–H bond is broken. Agostic bonds have since commonly been reported on the basis of NMR characterization alone.⁵

Many three-center-bonded complexes, particularly those in which the bond is unsupported, are unstable, reactive, and

- (1) Brookhart, M.; Green, M. L. H. *J. Organomet. Chem.* **1983**, *250*, 395.
- (2) (a) Muetterties, E. L. *Chem. Soc. Rev.* **1983**, *12*, 283. (b) Jones, W. D.; Feher, F. J. *J. Am. Chem. Soc.* **1984**, *106*, 1650. (c) Saillard, J.-Y.; Hoffmann R. *J. Am. Chem. Soc.* **1984**, *106*, 2006. (d) Eisenstein, O.; Jean, Y. *J. Am. Chem. Soc.* **1985**, *107*, 1177. (e) Crabtree, R. H. *Chem. Rev.* **1985**, *85*, 245. (f) Lichtenberger, D. L.; Kellogg, G. E. *J. Am. Chem. Soc.* **1986**, *108*, 2560. (g) Crabtree, R. H.; Hamilton, D. G. *Adv. Organomet. Chem.* **1988**, *28*, 299. (h) Morse, J. M.; Parker, G. H.; Burke, T. J. *Organometallics* **1989**, *8*, 2471. (i) Crabtree, R. H. *Angew. Chem., Int. Ed. Engl.* **1993**, *32*, 789. (j) Song, J.; Hall, M. B. *Organometallics* **1993**, *12*, 3118. (k) Nicholls, J. C.; Spencer, J. L. *Organometallics* **1994**, *13*, 1781. (l) Bengali, A. A.; Schultz, R. H.; Moore, C. B.; Bergman, R. G. *J. Am. Chem. Soc.* **1994**, *116*, 9585. (m) Arndtsen, B. A.; Bergman, R. G.; Mobley, T. A.; Peterson, T. H. *Acc. Chem. Res.* **1995**, *28*, 154. (n) Arndtsen, B. A.; Bergman, R. G. *Science* **1995**, *270*, 1970. (o) Schneider, J. J. *Angew. Chem., Int. Ed. Engl.* **1996**, *35*, 1068. (p) Hall, C.; Perutz, R. N. *Chem. Rev.* **1996**, *96*, 3125. (q) Ashbury, J. B.; Ghosh, H. N.; Yeston, J. S.; Bergman, R. G.; Lian, T. *Organometallics* **1998**, *17*, 3417.
- (3) Brookhart, M.; Green, M. L. H.; Wong, L.-L. *Prog. Inorg. Chem.* **1988**, *36*, 1.

- (4) (a) Schultz, A. J.; Williams, J. M.; Schrock, R. R.; Rupprecht, G. A.; Fellman, J. D. *J. Am. Chem. Soc.* **1979**, *101*, 1593. (b) Brown, R. K.; Williams, J. M.; Schultz, A. J.; Stucky, G. D.; Ittel, S. D.; Harlow, R. L. *J. Am. Chem. Soc.* **1980**, *102*, 981. (c) Beno, M. A.; Williams, J. M.; Tachikawa, M.; Muetterties, E. L. *J. Am. Chem. Soc.* **1981**, *103*, 1485. (d) Schultz, A. J.; Teller, R. G.; Beno, M. A.; Williams, J. M.; Brookhart, M.; Lamanna, W.; Humphrey, M. B. *Science* **1983**, *220*, 197. (e) Cracknell, R. B.; Orpen, A. G.; Spencer, J. L. *J. Chem. Soc., Chem. Commun.* **1984**, 326. (f) Carr, N.; Dunne, B. J.; Orpen, A. G.; Spencer, J. L. *J. Chem. Soc., Chem. Commun.* **1988**, 926. (g) Jordan, R. F.; Bradley, P. K.; Baenziger, N. C.; LaPointe, R. E. *J. Am. Chem. Soc.* **1990**, *112*, 1289. (h) Feng, S. G.; White, P. S.; Templeton, J. L. *J. Am. Chem. Soc.* **1990**, *112*, 8192. (i) Hyla-Kryspin, I.; Gleiter, R.; Krüger, C.; Zwettler, R.; Erker, G. *Organometallics* **1990**, *9*, 517. (j) Conroy-Lewis, F. M.; Mole, L.; Redhouse, A. D.; Lister, S. A.; Spencer, J. L. *J. Chem. Soc., Chem. Commun.* **1991**, 1601. (k) Albéniz, A. C.; Schulte, G.; Crabtree, R. H. *Organometallics* **1992**, *11*, 242. (l) Kündig, E. P.; Amurrio, D.; Bernardinelli, G.; Chowdhury, R. *Organometallics* **1993**, *12*, 4275. (m) Kuhlman, R.; Streib, K.; Caulton, K. G. *J. Am. Chem. Soc.* **1993**, *115*, 5813. (n) Poole, A. D.; Williams, D. N.; Kenwright, A. M.; Gibson, V. C.; Clegg, W.; Hockless, D. C. R.; O'Neill, P. A. *Organometallics* **1993**, *12*, 2549. (o) Braga, D.; Grepioni, F.; Biradha, K.; Desiraju, G. R. *J. Chem. Soc., Dalton Trans.* **1996**, 3925.

difficult to isolate, and for these compounds, NMR spectroscopy may be the only readily available method by which these bonds can be detected. An understanding of how the coupling constant is influenced by changes (in ligands and/or coordination geometry) occurring at the metal is likely to be of value in the design of complexes that are effective in activating C–H bonds.

The activation of Si–H⁶ and Sn–H⁷ bonds occurs in a manner apparently similar to that of C–H bonds but is, in many cases, more readily observable (the presence of d orbitals stabilizes the interaction to some extent). The decrease in $J(\text{Si–H})$, on complexation of R₃SiH to a transition metal, to a value intermediate between those of free R₃SiH and fully complexed R₃SiH (i.e., R₃Si–M–H) has been noted by Corriu^{6c} and Schubert,⁶ⁱ and there is clear evidence that a similar relationship holds in the case of tin.⁷ The advantages of working with tin are the higher stability of its three-center-bonded complexes relative to those of carbon and silicon and the higher natural abundance of its NMR-active isotopes (¹¹⁷Sn, ¹¹⁹Sn).

An E–H (E = C, Si, Sn) spin-coupling constant (potentially) provides information of a more specific nature than that of simply the presence or absence of a three-center bond: the strength of a three-center bond is undoubtedly reflected in some way by $J(\text{E–H})$. Here problems immediately arise, since an NMR spin-coupling constant is a function of a number of variables not all of which are related to the strength of the bond(s) between the coupled nuclei. It would be useful to know how the value of $J(\text{E–H})$ responds to changes made (in, for example, the nucleophilicity of ligands) to the coordination sphere of the transition metal and whether the effects of changes in electron density available to the three atoms forming the three-center bond can be distinguished from other factors (e.g., the s character of the bond between the coupled nuclei and the energy

difference between electronic ground and excited states) in determining the value of J .

A step in this direction was taken in a previous study in this area,^{7b} in which an activation enthalpy (~96 kJ mol⁻¹) was measured for the dissociation of Ph₃SnH from the complex [Rh(NCBPh₃)(H)(SnPh₃)(PPh₃)(4-Me₂Npy)], for which $J(\text{Sn–H}) = 106$ Hz. Complexes with unsubstituted pyridine and 4-MeO₂Cpy in place of the more nucleophilic 4-Me₂Npy gave $J(\text{Sn–H})$ values of 99 and 95 Hz, respectively. The related complex [Rh(NCBPh₃)(H)(SnPh₃)(PPh₃)₂] was shown by an X-ray study, by observation of its thermal stability, and by its tin–hydrogen coupling constant ($J(\text{Sn–H}) = 29$ Hz) to be much closer to the full oxidative addition limit.

The E–H coupling constant is only one of a number of NMR parameters that are potentially accessible for a three-center-bonded system. In the present study, chemical shifts and coupling constants for the nuclei ¹H, ³¹P, ¹⁰³Rh, and ¹¹⁹Sn are measured for over 50 compounds in an attempt, within a fairly narrow range of rhodium chemistry, to correlate NMR data with chemical properties that might be expected to influence the strength of a three-center bond.

Experimental Section

Materials. [Rh(Cl)(PPh₃)₃],⁸ [Rh(Cl){P(4-C₆H₄F)₃}₃],⁸ [Rh₂(Cl)₂(C₂H₄)₄],⁹ [Rh(NCBPh₃)(PPh₃)₃],^{10a} [Rh(N(CN)₂)(PPh₃)₃],^{10b} [Rh(N₃)(PPh₃)₃] (using NaN₃ in place of LiN₃),¹¹ and [Rh(O₂-CCF₃)(PPh₃)₃] (reaction in hexane rather than ethanol)¹² were prepared by published methods. [Rh(NCO)(PPh₃)₃] and [Rh(NCS)(PPh₃)₃] were prepared from [Rh(Cl)(PPh₃)₃] by metathesis with KOCN in ethanol or KSCN in benzene/ethanol (with a large excess of PPh₃) and shown by ¹⁵N NMR spectroscopy to have the NCX ligand bound to rhodium via nitrogen.¹³ [Rh(Cl){P(4-C₆H₄Me)₃}₃] was prepared in situ in ~0.04 M concentration in dichloromethane (0.5 mL) from [Rh₂(Cl)₂(C₂H₄)₄] (4 mg) and P(4-C₆H₄Me)₃ (18 mg); the solution was centrifuged to remove traces of undissolved solid. For NMR measurements, the following were prepared in situ in 0.03–0.04 M concentrations in ~5% CD₂Cl₂/CH₂Cl₂ (0.5 mL): *trans*-[Rh(NCBPh₃)(H)(SnPh₃)(PPh₃)₂(L)] (**3a**), from *trans*-[Rh(NCBPh₃)(H)(SnPh₃)(PPh₃)₂] (**1**) (20 mg) and L (~0.7 M or 10% volume if liquid), and *trans*-[Rh(X)(H)(SnPh₃)(PPh₃)₂(L)] (**3**), from [Rh(X)(PPh₃)₃] (15–20 mg), L (~0.7 M or 10% volume), and Ph₃SnH (~10 mg, ~0.05 M), both with cooling in a xylene slurry at ~ -50 °C, and [Rh(X)(H)(SnPh₃)(PPh₃)(L)] (**2**), from [Rh(X)(PPh₃)₃], L, and Ph₃SnH, with cooling in an ice/water bath. For X = Cl, complexes with P(4-C₆H₄F)₃ and P(4-C₆H₄Me)₃ in place of PPh₃ were prepared in a similar way, as was *cis*-[Rh(Cl)(H)(SnPh₃)(PR₃)₂(L)] (**4**).

Dichloromethane was distilled from P₂O₅, and pyridine and toluene were dried over CaH₂; other solvents and reagents were of the highest available purity and were used without further treatment. All solutions were prepared under an argon atmosphere.

NMR Spectroscopy. Spectra were recorded at 248 and 213 K on a Bruker DRX 400 spectrometer equipped with a 5 mm triple-resonance inverse probe with a dedicated ³¹P channel and

- (5) (a) Barreto, R. D.; Fehlner, T. P. *J. Am. Chem. Soc.* **1988**, *110*, 4471. (b) Cox, D. N.; Roulet, R. T. *J. Chem. Soc., Chem. Commun.* **1989**, 175. (c) Bennett, M. A.; Nicholls, J. C.; Rahman, A. K. F.; Redhouse, A. D.; Spencer, J. L.; Willis, A. C. *J. Chem. Soc., Chem. Commun.* **1989**, 1328. (d) Brookhart, M.; Lincoln, D. M.; Volpe, A. F.; Schmidt, G. F. *Organometallics* **1989**, *8*, 1212. (e) Erker, G.; Zwieter, R.; Krüger, C.; Hyla-Kryspin, I.; Gleiter, R. *Organometallics* **1990**, *9*, 524. (f) Brookhart, M.; Lincoln, D. M.; Bennett, M. A.; Pelling, S. J. *Am. Chem. Soc.* **1990**, *112*, 2691. (g) Bullock, R. M.; Lemke, F. R.; Szalda, D. J. *J. Am. Chem. Soc.* **1990**, *112*, 3244. (h) Bower, D. K.; Keister, J. B. *Organometallics* **1990**, *9*, 2321. (i) Etienne, M.; White, P. S.; Templeton, J. L. *J. Am. Chem. Soc.* **1991**, *113*, 2324. (j) Ogasawara, M.; Aoyagi, K.; Saburi, M. *Organometallics* **1993**, *12*, 3393. (k) Spencer, J. L.; Mhinzi, G. S. *J. Chem. Soc., Dalton Trans.* **1995**, 3819. (l) Geftakis, S.; Ball, G. E. *J. Am. Chem. Soc.* **1998**, *120*, 9953.
- (6) (a) Hart-Davis, A. J.; Graham, W. A. G. *J. Am. Chem. Soc.* **1971**, *93*, 4388. (b) Schubert, U.; Ackermann, K.; Wörle, B. *J. Am. Chem. Soc.* **1982**, *104*, 7378. (c) Schubert, U.; Scholz, G.; Müller, J.; Ackermann, K.; Wörle, B.; Stansfield, R. F. D. *J. Organomet. Chem.* **1986**, *306*, 303. (d) Colomer, E.; Corriu, R. J. P.; Marzin, C.; Vioux, A. *Inorg. Chem.* **1982**, *21*, 368. (e) Carré, F.; Colomer, E.; Corriu, R. J. P.; Vioux, A. *Organometallics* **1984**, *3*, 1272. (f) Graham, W. A. G. *J. Organomet. Chem.* **1986**, *300*, 81. (g) Schubert, U.; Bahr, K.; Müller, J. *J. Organomet. Chem.* **1987**, *327*, 357. (h) Schubert, U.; Müller, J.; Alt, H. G. *Organometallics* **1987**, *6*, 469. (i) Schubert, U. *Adv. Organomet. Chem.* **1990**, *30*, 151. (j) Luo, X.-L.; Kubas, G. J.; Bryan, J. C.; Burns, C. J.; Unkefer, C. J. *J. Am. Chem. Soc.* **1994**, *116*, 10312. (k) Luo, X.-L.; Kubas, G. J.; Burns, C. J.; Bryan, J. C.; Unkefer, C. J. *J. Am. Chem. Soc.* **1995**, *117*, 1159. (l) Kim, Y.-J.; Lee, S.-C.; Park, J.-I.; Osakada, K.; Choi, J.-C.; Yamamoto, T. *Organometallics* **1998**, *17*, 4929.
- (7) (a) Cardin, C. J.; Cardin, D. J.; Parge, H. E.; Power, J. M. *J. Chem. Soc., Chem. Commun.* **1984**, 609. (b) Schubert, U.; Kunz, E.; Harkers, B.; Willnecker, J.; Meyer, J. *J. Am. Chem. Soc.* **1989**, *111*, 2572. (c) Piana, H.; Kirchgässner, U.; Schubert, U. *Chem. Ber.* **1991**, *124*, 743. (d) Schubert, U.; Schubert, J. *J. Organomet. Chem.* **1992**, *434*, 169. (e) Schubert, U.; Gilbert, S.; Mock, S. *Chem. Ber.* **1992**, *125*, 835. (f) Carlton, L.; Weber, R. *Inorg. Chem.* **1993**, *32*, 4169. (g) Gilbert, S.; Knorr, M.; Mock, S.; Schubert, U. *J. Organomet. Chem.* **1994**, *480*, 241. (h) Carlton, L.; Weber, R.; Levendis, D. C. *Inorg. Chem.* **1998**, *37*, 1264.

(8) Osborn, J. A.; Wilkinson, G. *Inorg. Synth.* **1967**, *10*, 67.

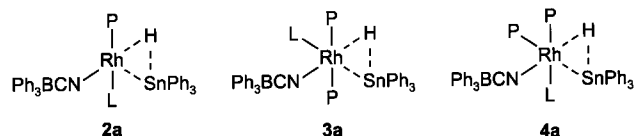
(9) Cramer, R. *Inorg. Synth.* **1974**, *15*, 14.

(10) (a) Carlton, L.; Weber, R. *Inorg. Chem.* **1996**, *35*, 5843. (b) Carlton, L.; Weber, R. *Magn. Reson. Chem.* **1997**, *35*, 817.

(11) Beck, W.; Fehlhämmer, W. P.; Pöllmann, P.; Schächl, H. *Chem. Ber.* **1969**, *102*, 1976.

(12) Robinson, S. D.; Uttley, M. F. *J. Chem. Soc., Dalton Trans.* **1973**, 1912.

(13) Carlton, L. Paper in preparation.

Chart 1. Complexes Formed by Reaction of **1** with L (P = PPh₃)

extended decoupler range, operating at 400.13 MHz (¹H), 161.98 MHz (³¹P), 12.65 MHz (¹⁰³Rh), and 149.21 MHz (¹¹⁹Sn). Two-dimensional ¹⁰³Rh–³¹P spectra were obtained using the pulse sequence $\pi/2(^{31}\text{P}) - 1/[2J(^{103}\text{Rh}-^{31}\text{P})] - \pi/2(^{103}\text{Rh}) - \tau - \pi(^{31}\text{P}) - \tau - \pi/2(^{103}\text{Rh}) - \text{Acq}(^{31}\text{P})$.¹⁴ A spectral width in f2 (³¹P) of 8 ppm and an acquisition time of 0.396 s gave a digital resolution of 1.26 Hz/point; in f1 (¹⁰³Rh), a spectral width of 40 ppm (increased in a few cases, where the signal was poorly resolved, to 100 or 200 ppm) and a time domain of 256 (reduced, in some cases, to ~100) gave, after zero filling, a digital resolution of 0.49 Hz/point. With a relaxation delay of 1 s and 4 scans per increment (in some cases increased to 8 or 16), data collection required 27 min. To eliminate the possibility of a folded signal in f1, spectra were first recorded with a spectral width of 2000 ppm.

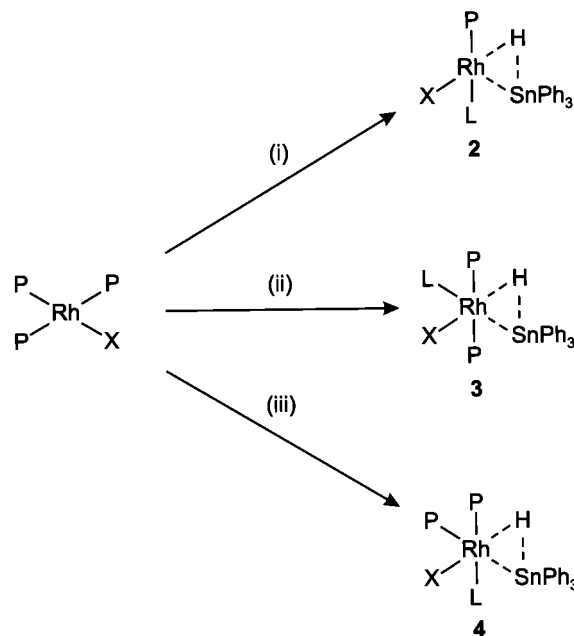
Chemical shifts were referenced to the generally accepted standards of H₃PO₄, $\Xi(^{103}\text{Rh}) = 3.16$ MHz,¹⁵ and SnMe₄, with negative values indicating shielding. The chemical shifts of H₃PO₄ (85%, 300 K) and SnMe₄ (neat liquid, 248 K) with a CD₂-Cl₂ external lock correspond to frequencies of 161.975 500 and 149.210 995 MHz, respectively, in a field (4.395 T) in which the protons of TMS (in CD₂Cl₂ at 300 K) resonate at 400.130 020 MHz.

With the exception of complexes containing trifluoroacetate, which, for reasons of stability, were dissolved in toluene, all compounds were studied in solution in dichloromethane. To allow a meaningful comparison between the data obtained using the two solvents, a correction was applied to the trifluoroacetate data based on measurements from [Rh(NCO)(H)(SnPh₃)(PPh₃)(py)], for which $\delta(^{119}\text{Sn})$ and $\delta(^{103}\text{Rh})$ are –132.4 and 1267 ppm, respectively, in dichloromethane and –130.7 and 1287 ppm, respectively, in toluene (all at –25 °C).

The effect on chemical shifts of varying the concentration of L was measured for [Rh(Cl)(H)(SnPh₃)(PPh₃)(py)] (**2gy**). Upon an increase in the concentration of pyridine from 10% to 30%, the changes observed were $\delta(^1\text{H}) + 0.14$, $\delta(^{31}\text{P}) - 0.09$, $\delta(^{103}\text{Rh}) + 0.6$, and $\delta(^{119}\text{Sn}) - 0.05$ ppm. No changes were detectable on reducing the concentration of pyridine to 5%.

Results and Discussion

Complexes Studied. The complex *trans*-[Rh(NCBPh₃)(H)(SnPh₃)(PPh₃)₂] (**1**), which can be readily prepared in good yield,¹⁰ is a precursor of a number of compounds containing pyridine and substituted pyridines. In solution in dichloromethane or toluene at room temperature, **1** reacts with L (L: 4-carbomethoxypyridine, 4-MeO₂Cpy, **x**; pyridine, py, **y**; 4-(dimethylamino)pyridine, 4-Me₂Npy, **z**) to give **2a**^{7h} (Chart 1). In solutions prepared at ~–50 °C, **3a** is formed as the only product, which, on standing at –25 °C, undergoes slow conversion to **4a** and other products.^{7h} In solution, complexes

Scheme 1. Reactions of [RhX(PPh₃)₃] with L and Ph₃SnH in Dichloromethane^a

^a (i) Complexes **2** at 0 or 22 °C: X = NCBPh₃ (**a**), N(CN)₂ (**b**), NCS (**c**), N₃ (**d**), NCO (**e**), O₂CCF₃ (**f**), Cl/PPh₃ (**g**), Cl/P(C₆H₄F)₃ (**g'**), Cl/P(C₆H₄Me)₃ (**g''**); L = 1-Meim (**w**), 4-MeO₂Cpy (**x**), py (**y**), 4-Me₂Npy (**z**); P = PPh₃. (ii) Complexes **3** at –25 °C: X = **a**, **b**, **c**, **e**, **g**, **g'**, **g''**; L = **x**, **y**, **z** (**x**, **y** only for **g**–**g''**), 4-MeCOC₆H₄CN (**r**), C₆H₅CN (**s**), 4-Me₂NC₆H₄CN (**t**). (iii) Complexes **4** at 0 °C: X = **g**, **g'**, **g''**; L = **r**, **s**, **t**.

2a–4a are less stable than **1**, all studies being carried out on samples prepared in situ at temperatures of 0 °C and below.

Complexes **2a–4a** can also be prepared from [Rh(NCBPh₃)(PPh₃)₃] and Ph₃SnH in solutions containing L, again without isolation in solid form. This method was used to prepare a series of analogues of **2** (also of **3** and **4**; see below) in which ligands X, L, and, for X = Cl, the phosphine were independently varied (Scheme 1, Figure 1). The low solubility of (dimethylamino)pyridine in toluene precluded studies of **2fz** (X = trifluoroacetate). Reactions with methylimidazole (1-Meim, **w**) give, with X = N(CN)₂, NCO, and N₃, a second, unidentified, product in which group X has been lost. With X = Cl and O₂CCF₃, this is the only major tin-containing product; the desired products, **2fw** and **2gw**, are not formed.

In solutions prepared at temperatures of –25 °C or below, product **3** is formed (Scheme 1) in some, but not all, cases. With L = 4-Me₂Npy, **3** is formed only with X = NCBPh₃, N(CN)₂, NCS, and NCO (complexes **3az–cz, ez**). With L = 1-Meim, a product (**3aw**) is formed in good yield only in the case for X = NCBPh₃ (starting from **1**) where precipitation (as a white microcrystalline powder) prevented the recording of an ¹¹⁹Sn spectrum. With L = py, **3ay** is isolated as a very pale yellow powder at –50 °C using hexane. **3aw** and **3ay** are obtained in slightly impure form in 60–70% yield and are stable, in the solid state, at room temperature. The concentration of **3** can be increased by the addition of triphenylphosphine; data for **3bz** and **3cz** were obtained under this condition. With X = NCS and L = 4-MeO₂Cpy (**3cx**), a thick cream-colored precipitate is slowly formed.

In spectra of **3** recorded at –25 °C, the ¹H signal (Figure 1a) shows slight to moderate broadening and the ¹¹⁹Sn signal severe broadening (Figure 1d) where X = N(CN)₂, NCO, NCS, and Cl. At –60 °C, the spectral lines are well resolved (Figure 1e).

(14) Bax, A.; Griffey, R. H.; Hawkins, B. L. *J. Magn. Reson.* **1983**, *55*, 301.

(15) Kidd, R. G.; Goodfellow, R. J. In *NMR and the Periodic Table*; Harris, R. K., Mann, B. E., Eds.; Academic Press: London, 1978; pp 244–249.

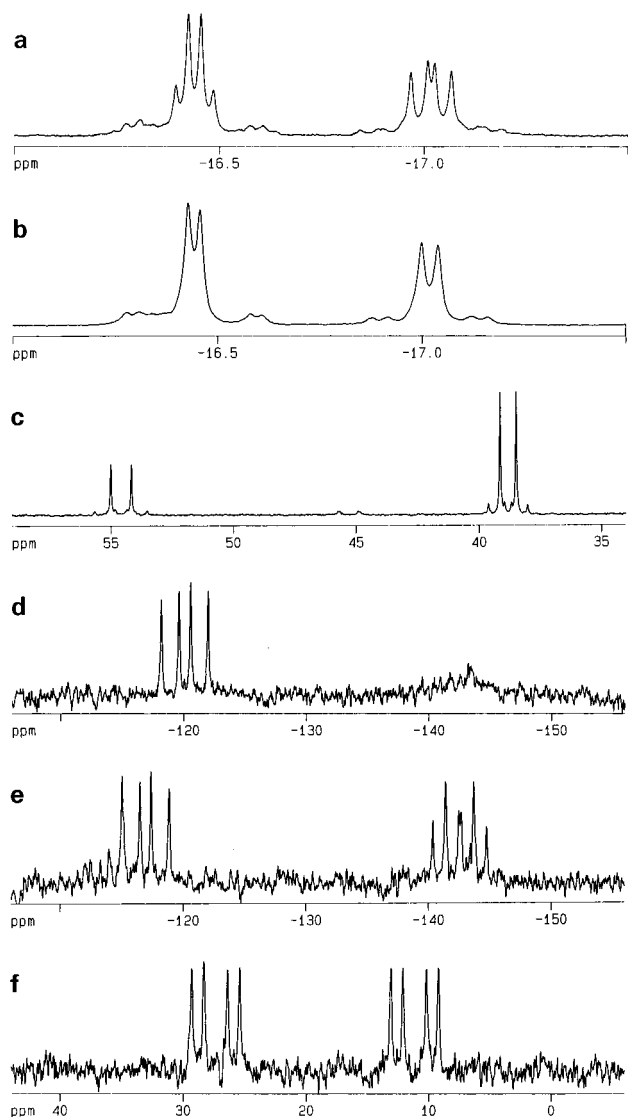


Figure 1. ^1H (a), $^1\text{H}\{^{31}\text{P}\}$ (b), $^{31}\text{P}\{^1\text{H}\}$ (c), $^{119}\text{Sn}\{^1\text{H}\}$ (d–f) spectra. Spectra a–e were recorded for a mixture of $[\text{Rh}(\text{N}(\text{CN})_2)(\text{PPh}_3)_3]$ (0.03 M), 4-MeO₂Cpy (0.5 M), and Ph_3SnH (0.05 M) in dichloromethane (prepared at $< -25^\circ\text{C}$) giving $[\text{Rh}(\text{N}(\text{CN})_2)(\text{H})(\text{SnPh}_3)(\text{PPh}_3)(4\text{-MeO}_2\text{-Cpy})]$ (**2bx**) and *trans*- $[\text{Rh}(\text{N}(\text{CN})_2)(\text{H})(\text{SnPh}_3)(\text{PPh}_3)_2(4\text{-MeO}_2\text{Cpy})]$ (**3bx**); spectra a–d were recorded at -25°C , and spectrum e was recorded at -60°C . Spectrum f was recorded at -25°C for a mixture of $[\text{Rh}(\text{Cl})\{\text{P}(\text{C}_6\text{H}_4\text{F})_3\}_3]$ (0.03 M), 4-Me₂NC₆H₄CN (0.5 M), and $\text{Ph}_3\text{-SnH}$ (0.05 M) in dichloromethane giving *cis*- $[\text{Rh}(\text{Cl})(\text{H})(\text{SnPh}_3)\{\text{P}(\text{C}_6\text{H}_4\text{F})_3\}_2(4\text{-Me}_2\text{NC}_6\text{H}_4\text{CN})]$ (**4g't**).

At -60°C , tin–hydrogen coupling constants for **3** are up to 8 Hz larger than those measured at -25°C (no further increase was found on going to -70°C), indicating that ligand L is quite labile (tin has a large trans effect), and at the higher temperature, $J(\text{Sn}–\text{H})$ is a weighted average of the values for complexes with and without ligand L.

The reaction of $[\text{RhCl}(\text{PR}_3)_3]$ with Ph_3SnH in the presence of benzonitrile gives, not **2** or **3**, but **4** (Scheme 1, Figure 1f), formed via what appears to be *trans*- $[\text{RhCl}(\text{H})(\text{SnPh}_3)(\text{PR}_3)_2]$ ($J(\text{Sn}–\text{H}) \sim 30$ Hz). Attempts to prepare **2** and **3** with L = PMePh_2 , PMe_3 , and $\text{P}(\text{OMe})_3$ from **1** with ≤ 1 equiv of L were unsuccessful, giving mixtures of unidentified products.

NMR Parameters. A listing of NMR data for the compounds studied is given in Table 1. The nuclei most informative about changes in Rh–H–Sn bonding are ^{103}Rh and ^{119}Sn , and discussion will be restricted to the parameters $\delta(^{103}\text{Rh})$, $\delta(^{119}\text{Sn})$, $J(^{119}\text{Sn}–^1\text{H})$, and $J(^{103}\text{Rh}–^{119}\text{Sn})$. Unfortunately no

single scale exists by which to quantify the electron-donating/withdrawing power of the ligands and functional groups used in the present study. The species $-\text{Me}$, $-\text{F}$, $-\text{CO}_2\text{Me}$, $-\text{COMe}$, and $-\text{NMe}_2$ are included in the Hammett scale;¹⁶ other scales dealing more specifically with ligands in metal complexes are based on carbonyl stretching frequencies¹⁷ or redox potentials.¹⁸ To avoid the problems associated with quantification of this variable, the data in the present study are presented in graphs with NMR parameters on both axes. More specifically, $J(\text{Sn}–\text{H})$ is plotted as a function of $\delta(^{119}\text{Sn})$, $\delta(^{103}\text{Rh})$, and $J(^{103}\text{Rh}–^{119}\text{Sn})$. The electron-donating/withdrawing dimension emerges of its own accord from this treatment of the data.

Factors Influencing Chemical Shifts. The rhodium chemical shift is determined principally by two terms in the Ramsey equation:^{19,20} ΔE^{-1} , where ΔE is the average energy difference between filled and empty d orbitals, and $\langle r^{-3} \rangle_d$ where r is the average radius of a valence level d orbital. ΔE is influenced by weak/strong properties of ligands and increases according to the spectrochemical series; r is influenced by hard/soft properties and increases according to the nephelauxetic series.^{20,21} Weak hard ligands cause a shift in $\delta(^{103}\text{Rh})$ to high δ , and strong soft ligands cause a shift to low δ . For weak soft ligands, where the two effects oppose each other, and for ligands that occupy a position toward the middle of each scale, such as pyridine, the influence on $\delta(^{103}\text{Rh})$ may be difficult to predict. In general, for weak ligands the $\langle r^{-3} \rangle$ term is dominant and for strong ligands the ΔE^{-1} term is dominant.²¹

Subject to these constraints, a change in the nucleophilicity of one or more of the ligands (X, L, P) attached to rhodium would be expected to have an influence on $\delta(^{103}\text{Rh})$ in the absence of any interaction with triphenyltin hydride.²² The presence of such an interaction, which is itself sensitive to changes in the electron density on rhodium, would further modify the influence (of changes in X, L, and P) on $\delta(^{103}\text{Rh})$.

The influences on the tin chemical shift are less numerous in the systems of the present study. The substituents on tin are limited to rhodium, hydrogen, and three phenyl groups, the rhodium fulfilling the role of a substituent of variable electron density. The effect on $\delta(^{119}\text{Sn})$ of an increase in the electron density on tin has been shown for the series of compounds $\text{Me}_3\text{SnCH}_3\text{-}n\text{Cl}_n$ ($n = 0–3$) to be a decrease from +85 to 0 ppm²³ (the authors use the opposite sign convention) and for $[\text{Rh}(\text{SnCl}_3)_2(1,5\text{-cod})\{\text{P}(\text{C}_6\text{H}_4\text{R})_3\}]^-$ a decrease from +44.1 to +34.8 ppm as R is varied in the order F, Cl, H, OMe.²⁴ A change in the tin coordination number from 4 to 5 also causes a negative shift in $\delta(^{119}\text{Sn})$.²⁵

Signs of Coupling Constants. In a two-dimensional (X–Y correlated) spectrum showing “passive” coupling to a third nucleus (Z), the tilt of the cross-peaks provides information about the relative signs of $J(\text{X}–\text{Z})$ and $J(\text{Y}–\text{Z})$. Where nuclei

- (16) (a) Jaffe, H. H. *Chem. Rev.* **1953**, *53*, 191. (b) McDaniel, D. H.; Brown, H. C. *J. Org. Chem.* **1958**, *23*, 420. (c) Wells, P. R. *Chem. Rev.* **1963**, *63*, 171.
 (17) Tolman, C. A. *Chem. Rev.* **1977**, *77*, 313.
 (18) Chatt, J.; Kan, C. T.; Leigh, G. J.; Pickett, C. J.; Stanley, D. R. *J. Chem. Soc., Dalton Trans.* **1980**, 2032.
 (19) Ramsey, N. F. *Phys. Rev.* **1950**, *78*, 699; **1952**, *86*, 243.
 (20) Mason, J. *Chem. Rev.* **1987**, *87*, 1299.
 (21) Mann, B. E. In *Transition Metal NMR*; Pregosin, P. S., Ed.; Elsevier: Amsterdam, 1991; pp 177–215.
 (22) (a) Elsevier, C. J.; Kowall, B.; Kragten, H. *Inorg. Chem.* **1995**, *34*, 4836. (b) Carlton, L. *Magn. Reson. Chem.* **1997**, *35*, 153.
 (23) Davies, A. G.; Harrison, P. G.; Kennedy, J. D.; Mitchell, T. N.; Puddephatt, R. J.; McFarlane, W. *J. Chem. Soc. C* **1969**, 1136.
 (24) Kretschmer, M.; Pregosin, P. S.; Garralda, M. *J. Organomet. Chem.* **1983**, *244*, 175.
 (25) Wrackmeyer, B. *Annu. Rep. NMR Spectrosc.* **1985**, *16*, 73.

<i>trans</i> -[Rh(CI)(H)(SnPh ₃)(P(C ₆ H ₄ F) ₃) ₂ (py)] (3g'y)	579	13.1	18.1	126	108.4	171	342
<i>trans</i> -[Rh(CI)(H)(SnPh ₃)(P(C ₆ H ₄ Me) ₃) ₂ (4-MeO ₂ Cpy)] (3g'x)	607	12.9	17.9	125	106.1	167	350
<i>trans</i> -[Rh(CI)(H)(SnPh ₃)(P(C ₆ H ₄ Me) ₃) ₂ (py)] (3g'y)	606	12.6	18.0	130	106.3	172	358
<i>cis</i> -[Rh(CI)(H)(SnPh ₃)(PPh ₃) ₂ (4-MeCOC ₆ H ₄ CN)] (4gr) ^k	171	4.1	14.0	80	109.4	2378	435
	37.07	14.4			92.5	151	
	36.26	<1	14.1	82	109.7	2397	444
<i>cis</i> -[Rh(CI)(H)(SnPh ₃)(PPh ₃) ₂ (C ₆ H ₅ CN)] (4gs) ^k		14.4			92.3	154	
	36.01	3.9	13.9	85	110.5	2433	443
<i>cis</i> -[Rh(CI)(H)(SnPh ₃)(PPh ₃) ₂ (4-Me ₂ NC ₆ H ₄ CN)] (4gt) ^k		13.9			91.6	158	
	35.52	5.4	14.5	74	109.7	2361	426
<i>cis</i> -[Rh(CI)(H)(SnPh ₃)(P(C ₆ H ₄ F) ₃) ₂ (4-MeCOC ₆ H ₄ CN)] (4gr) ^k	177	14.8			92.0	145	
	33.51	5.2	14.5	76	110.2	2380	429
<i>cis</i> -[Rh(CI)(H)(SnPh ₃)(P(C ₆ H ₄ F) ₃) ₂ (C ₆ H ₅ CN)] (4gs) ^k		14.7			92.1	145	
	34.89	5.1	14.4	80	110.8	2417	443
<i>cis</i> -[Rh(CI)(H)(SnPh ₃)(P(C ₆ H ₄ F) ₃) ₂ (4-Me ₂ NC ₆ H ₄ CN)] (4gt) ^k	213	14.4			91.7	147	
	34.54	4.2	13.9	88	112.0	2458	442
<i>cis</i> -[Rh(CI)(H)(SnPh ₃)(P(C ₆ H ₄ Me) ₃) ₂ (4-Me ₂ NC ₆ H ₄ CN)] (4gt) ^k	217	18.46			91.5	155	
	35.50	13.9					
	33.96						

^a Solution (0.03–0.04 M) in CD₂Cl₂/CH₂Cl₂. ^b Chemical shifts in ppm from TMS (internal standard). ^c Chemical shifts in ppm from a frequency defined by H₃PO₄ (external standard) at 300 K. ^d Chemical shifts in ppm from E = 3.16 MHz. ^e Chemical shifts in ppm from a frequency defined by SnMe₄ (external standard) at 248 K. ^f Coupling constants (absolute magnitude) in Hz. Signs are probably as follows: ²J(Sn–H_{cis}), ²J(Sn–P_{cis}), and ¹J(Rh–Sn) positive; ¹J(Rh–H), ¹J(Rh–H), ¹J(Rh–H), ¹J(Rh–H), ¹J(Rh–H) negative. ^g J(¹¹⁹Sn–¹H) ~ J(¹¹⁷Sn–³¹P) was measured from the ¹¹⁹Sn spectrum. The value for **3aw** was measured from the ³¹P spectrum. ^h Data for **2ax–z** were taken from ref 7h. ⁱ J(Rh–H) for **2ax** was remeasured. ^j Solvent toluene. ^k J(³¹P–³¹P), Hz: **4gr**, 17.8; **4gs**, 17.8; **4gt**, 17.8; **4gr**, 17.6; **4gs**, 17.5; **4gt**, 17.2; **4gt**, 17.8.

X and Y both have positive gyromagnetic ratios (γ), a positive tilt (from lower left to upper right, the high- δ peaks in the X dimension correlating with the high- δ peaks in the Y dimension) indicates that $J(X-Z)$ and $J(Y-Z)$ have the same sign. In the case where γ_X and γ_Y have opposite signs, the situation is complicated by the fact that the precessional frequencies of X and Y also have opposite signs, a difference which is not reflected in the chemical shift scale. In a two-dimensional X–Y correlated spectrum obtained from nuclei having opposite signs of γ , a positive tilt of cross-peaks will indicate that $J(X-Z)$ and $J(Y-Z)$ have *opposite* signs. The signs of NMR frequencies and phases in relation to γ have been discussed by Levitt,²⁶ and the determination of the signs of coupling constants in transition metal complexes using 2D spectra has been described by Otting et al.²⁷

The nuclei observed in the 2D spectra shown in Figure 2 are ¹H and ³¹P (positive γ) and ¹¹⁹Sn and ¹⁰³Rh (negative γ). Accordingly, the positive tilt of the cross-peaks in Figure 2a (¹¹⁹Sn–¹H) indicates that $J(^{103}\text{Rh}-^{119}\text{Sn})$ and $J(^{103}\text{Rh}-^1\text{H})$ have opposite signs as do $J(^{119}\text{Sn}-^{31}\text{P})$ and $J(^{31}\text{P}-^1\text{H})$; the positive tilt in Figure 2b (³¹P–¹H) indicates that $J(^{103}\text{Rh}-^{31}\text{P})$ and $J(^{103}\text{Rh}-^1\text{H})$ have the same sign as do $J(^{119}\text{Sn}-^{31}\text{P})$ and $J(^{119}\text{Sn}-^1\text{H})$; the negative tilt in Figure 2c (¹⁰³Rh–³¹P) indicates that $J(^{103}\text{Rh}-^{119}\text{Sn})$ and $J(^{119}\text{Sn}-^{31}\text{P})$ also have the same sign as do $J(^{103}\text{Rh}-^1\text{H})$ and $J(^{31}\text{P}-^1\text{H})$. The signs of both ¹J(¹⁰³Rh–¹H) and ¹J(¹⁰³Rh–³¹P) have been measured as negative.²⁸ From this and the data above, it is most likely that, for complexes **2** and **3**, ¹J(¹⁰³Rh–¹H), ¹J(¹⁰³Rh–³¹P), and ²J(³¹P–¹H_{cis}) are negative and ²J(¹¹⁹Sn–¹H_{cis}), ²J(¹¹⁹Sn–³¹P_{cis}), and ¹J(¹⁰³Rh–¹¹⁹Sn) are positive.

J(¹¹⁹Sn–¹H) as a Function of $\delta(^{119}\text{Sn})$. For complexes **2**, changes occur in $J(^{119}\text{Sn}-^1\text{H})$ and $\delta(^{119}\text{Sn})$ as ligand X is varied: these changes are shown in Figure 3 for pyridine-containing derivatives. Data points for complexes **2** define a gradient with $J(^{119}\text{Sn}-^1\text{H})$ increasing and $\delta(^{119}\text{Sn})$ decreasing, the sequence of points from lower left to upper right matching the order of increasing electron-donating ability of X. Data for **2**, X = Cl, lie ~ 14 ppm toward lower $\delta(^{119}\text{Sn})$ values than the data obtained with X = N-donor. A weak interaction between Cl and Sn could account for this difference. With L = 1-Meim and varied X, the data points for **2** give a line (not shown; the Meim data are described briefly elsewhere²⁹), of very similar gradient, lying ~6 ppm toward higher $\delta(^{119}\text{Sn})$ values than the line for X = NCBPh₃ etc. A change of the phosphine (X = Cl only) has an effect similar to that of changes in X, as shown also in Figure 3, where, with X = Cl, L = py, and varied phosphine (complex **2**), the three data points in order of increasing phosphine nucleophilicity lie approximately on a line parallel to that for varied X.

When the effects of varying ligand L are superimposed on this picture, lines shown in the lower portion of Figure 4b are obtained. With ligands X = NCBPh₃, N(CN)₂, NCS, N₃, and NCO, these lines are, to a good approximation, straight, having a gradient very similar, but not identical, to the gradient in Figure 3. With X = Cl, the lines show slight curvature but otherwise resemble the lines obtained with X = NCBPh₃, N(CN)₂, etc. In

(26) Levitt, M. H. *J. Magn. Reson.* **1997**, *126*, 164.

(27) Otting, G.; Soler, L. P.; Messerle, B. A. *J. Magn. Reson.* **1999**, *137*, 413.

(28) (a) Goggin, P. L.; Goodfellow, R. J.; Knight, J. R.; Norton, M. G.; Taylor, B. F. *J. Chem. Soc., Dalton Trans.* **1973**, 220. (b) Hyde, M. E.; Kennedy, J. D.; Shaw, B. L.; McFarlane, W. *J. Chem. Soc., Dalton Trans.* **1977**, 1571.

(29) Carlton, L. *Appl. Organomet. Chem.*, in press.

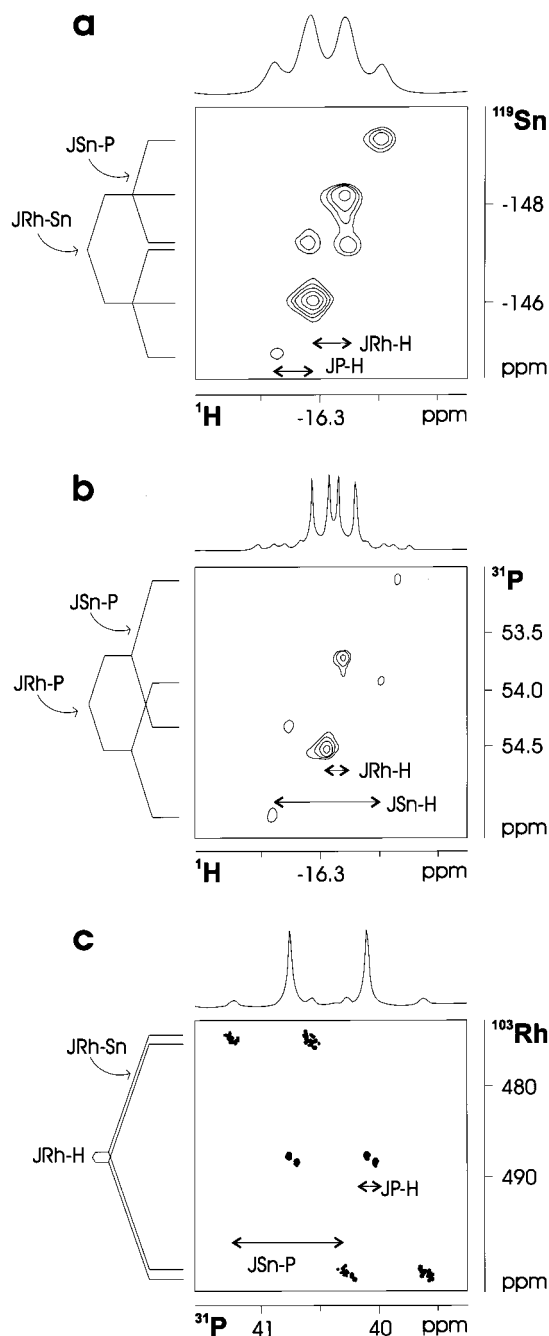


Figure 2. $^{119}\text{Sn}-^1\text{H}$ (a), $^{31}\text{P}-^1\text{H}$ (b) and $^{103}\text{Rh}-^{31}\text{P}$ (c) correlated spectra for *trans*-[Rh(NCBPh₃)(H)(SnPh₃)(PPh₃)₂(4-Me₂Npy)] (**3az**) (a and c) at $-60\text{ }^\circ\text{C}$ and for [Rh(NCBPh₃)(H)(SnPh₃)(PPh₃)(py)] (**2ay**) (b) at $-25\text{ }^\circ\text{C}$, showing passive coupling. The solvent was CD₂Cl₂. The main signal (center section) of spectrum c is shown at a much higher contour level than the Sn satellites. 1D spectra are external projections.

every case, the sequence in which the data points are ordered (from lower to upper) is from the least to the most nucleophilic pyridine.

When data ($J(^{119}\text{Sn}-^1\text{H})/\delta(^{119}\text{Sn})$) from the six-coordinate bis(phosphine) complexes **3** are included, lines in the upper portion of Figure 4b are obtained. Complexes **3** give higher $J(^{119}\text{Sn}-^1\text{H})$ and lower (i.e., more negative) $\delta(^{119}\text{Sn})$ values than **2**. Variation of ligand X and phosphine (X = Cl) causes a greater dispersion of data points in the $\delta(^{119}\text{Sn})$ dimension for **3** (as compared to **2**), and there is no clear relationship between $J(^{119}\text{Sn}-^1\text{H})/\delta(^{119}\text{Sn})$ and the electron-donating properties of X, in contrast to what is found for **2**. Variation of ligand L (pyridine)

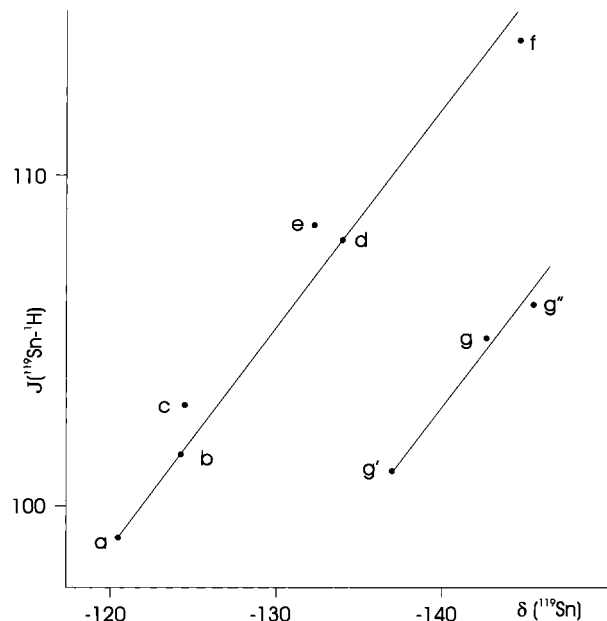


Figure 3. Plot of $J(^{119}\text{Sn}-^1\text{H})$ vs $\delta(^{119}\text{Sn})$ for the complexes [Rh(X)(H)(SnPh₃)(PPh₃)(L)] (**2**) with L = py and with X and phosphine (X = Cl only) varied: X = NCBPh₃ (a), N(CN)₂ (b), NCS (c), N₃ (d), NCO (e), O₂CCF₃ (f), Cl/PPh₃ (g), Cl/P(C₆H₄F)₃ (g'), Cl/P(C₆H₄Me)₃ (g''). Complexes were prepared in situ; the solvent was dichloromethane except for **2f** (toluene) where $\delta(\text{Sn})$ is corrected. Data were recorded at $-25\text{ }^\circ\text{C}$.

leads to a steeper $J(^{119}\text{Sn}-^1\text{H})/\delta(^{119}\text{Sn})$ gradient as compared to that for **2** with the trend toward lower $\delta(^{119}\text{Sn})$ values that accompanies increasing nucleophilicity of L reversed on exchange of 4-Me₂Npy for py. For a given ligand X, the data points for **3** (L = 4-MeO₂Cpy) lie on, or close to, the projection of the gradient for the relevant complexes **2**. The data for complexes **3ar-t** (X = NCBPh₃, L = benzonitriles) shown in Figure 4b closely match those for **2ax-z** (X = NCBPh₃, L = pyridines). However, upon variation of ligand X (work currently in progress), this apparent accord is lost.

The general trend in $\delta(^{119}\text{Sn})$ for complexes **2** and **3** (Figure 3) is reversed for **4** (not shown), which gives signals with δ values ~ 150 ppm higher than those for **2** or **3**. As the nucleophilicity of L (benzonitrile) is increased, both $J(^{119}\text{Sn}-^1\text{H})$ and $\delta(^{119}\text{Sn})$ increase. The effects of varying the phosphine are less clear. The similarities between the data for **2** and **3** clearly do not extend to **4**.

$J(^{119}\text{Sn}-^1\text{H})$ as a Function of $\delta(^{103}\text{Rh})$. A plot of $J(^{119}\text{Sn}-^1\text{H})$ vs $\delta(^{103}\text{Rh})$ is shown in Figure 5a for complex **2** with L = py and X varied. With L = Meim and X varied, a line (not shown) of similar gradient, lying ~ 150 ppm toward lower δ values, is obtained. The data point for the chloro complex (**2gy**) lies close to the line defined by the other X variants, in contrast to the findings shown in Figure 3 for $\delta(^{119}\text{Sn})$ data. Data for **3** (L = py, X varied; Figure 5b) give a line approximately parallel to that found for **2** (Figure 5a), indicating very similar responses to changes in X for the two series of compounds.

The rhodium chemical shifts for **2** are shown in Figure 5c (where the $\delta(^{103}\text{Rh})$ scale has been expanded relative to that in Figure 5a) for each ligand X, grouped according to the variation in pyridine. The gradient $J(^{119}\text{Sn}-^1\text{H})/\delta(^{103}\text{Rh})$ associated with changes in pyridine is much steeper (i.e., a smaller change in $\delta(^{103}\text{Rh})$ relative to $J(^{119}\text{Sn}-^1\text{H})$) than that associated with changes in X, in contrast to the $J(^{119}\text{Sn}-^1\text{H})/\delta(^{119}\text{Sn})$ data (Figure 3), where the effects of changing X and changing pyridine are very similar. The differing effects of X and L on

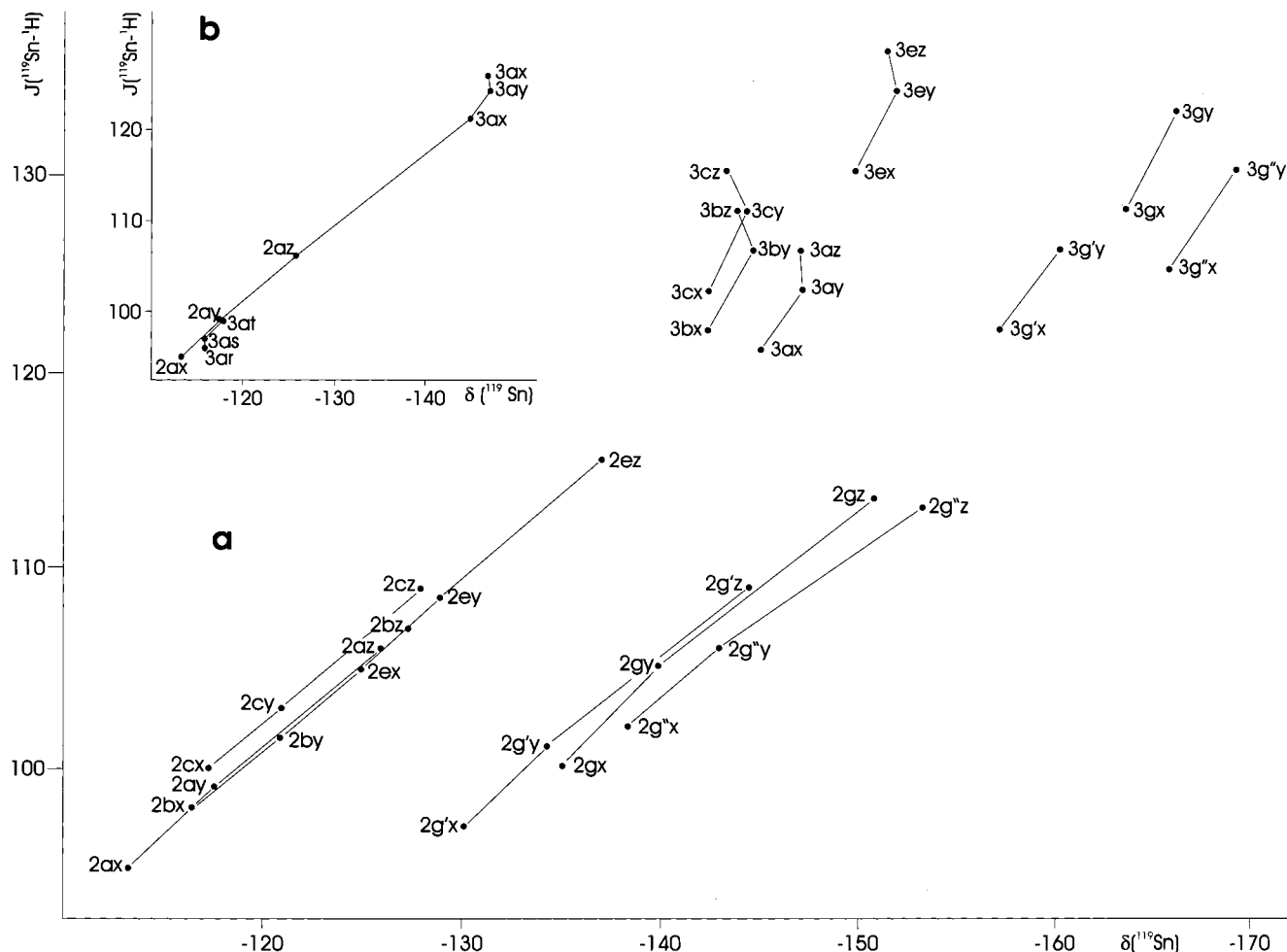


Figure 4. (a) Plot of $J(^{119}\text{Sn}-\text{H})$ vs $\delta(^{119}\text{Sn})$ for the complexes $[\text{Rh}(\text{X})(\text{H})(\text{SnPh}_3)(\text{PPh}_3)(\text{L})]$ (**2**) and $\text{trans}-[\text{Rh}(\text{X})(\text{H})(\text{SnPh}_3)(\text{PPh}_3)_2(\text{L})]$ (**3**) with X, phosphine (X = Cl only), and L varied: X = NCBPh₃ (a), N(CN)₂ (b), NCS (c), NCO (e), Cl/PPh₃ (g), Cl/P(C₆H₄F)₃ (g'), CP/P(C₆H₄Me)₃ (g''); L = 4-MeO₂Cpy (x), py (y), 4-Me₂Npy (z), 4-MeCOC₆H₄CN (r), C₆H₅CN (s), 4-Me₂NC₆H₄CN (t). Complexes were prepared in situ; the solvent was dichloromethane. Data were recorded at -60 °C. (b, Inset) Plot of $J(^{119}\text{Sn}-\text{H})$ vs $\delta(^{119}\text{Sn})$ for complexes **2a** and **3a** (dichloromethane, -60 °C).

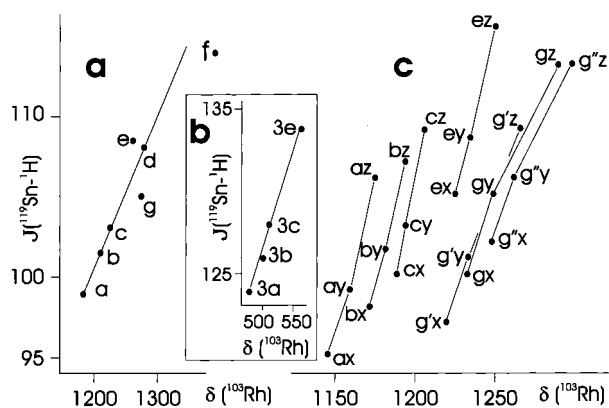


Figure 5. (a) Plot of $J(^{119}\text{Sn}-\text{H})$ vs $\delta(^{103}\text{Rh})$ for the complexes $[\text{Rh}(\text{X})(\text{H})(\text{SnPh}_3)(\text{PPh}_3)(\text{L})]$ (**2**) with L = py and X = NCBPh₃ (a), N(CN)₂ (b), NCS (c), N₃ (d), NCO (e), O₂CCF₃ (f). Data were recorded at -25 °C. (b) Plot of $J(^{119}\text{Sn}-\text{H})$ vs $\delta(^{103}\text{Rh})$ for the complexes $\text{trans}-[\text{Rh}(\text{X})(\text{H})(\text{SnPh}_3)(\text{PPh}_3)_2(\text{L})]$ (**3**) with L = py and X varied. Data were recorded at -60 °C. (c) Plot of $J(^{119}\text{Sn}-\text{H})$ vs $\delta(^{103}\text{Rh})$ for **2** with X, phosphine (X = Cl only), and L varied: L = 4-MeO₂Cpy (x), py (y), 4-Me₂Npy (z). Data were recorded at -60 °C. The solvent was dichloromethane except for **2f** (toluene) where $\delta(\text{Rh})$ is corrected. All complexes were prepared in situ.

$\delta(^{103}\text{Rh})$ are likely to reflect differing influences on ΔE and $\langle r^{-3} \rangle_d$ (see above). Changes in $\delta(^{103}\text{Rh})$ for **3** on varying L

(pyridines) are very small, amounting to no more than 0–2 ppm on replacing 4-MeO₂Cpy by py (X = NCBPh₃, N(CN)₂, NCS, NCO) and 6–7 ppm on replacing py by 4-Me₂Npy (Figure 6a). Much larger changes in $\delta(^{103}\text{Rh})$ are found for **3ar–t** (X = NCBPh₃, L = benzonitriles) on varying L (Figure 6b).

$J(^{119}\text{Sn}-\text{H})$ as a Function of $J(^{103}\text{Rh}-^{119}\text{Sn})$. A graph showing variations in $J(^{119}\text{Sn}-\text{H})$ and $J(^{103}\text{Rh}-^{119}\text{Sn})$ recorded for **2** and **3** in response to changes in ligand X (L = py; X varied) is given in Figure 7. The linear relationship holds also for **2** with L = 1-Meim and X varied but is rather less clear for L = MeO₂Cpy and Me₂Npy. Plots (not shown) of $J(^{119}\text{Sn}-\text{H})$ vs $J(^{103}\text{Rh}-^{119}\text{Sn})$ for **2** with L varied show gradients similar to those found with X varied. For **3**, the effects due to variations in L form no clear pattern.

NMR Data and Rh–H–Sn Bonding. Three features of the data from plots of $J(^{119}\text{Sn}-\text{H})$ vs $\delta(^{119}\text{Sn})$ and $\delta(^{103}\text{Rh})$ are particularly relevant to an interpretation of the Rh–H–Sn bonding.

(1) The response of $\delta(^{119}\text{Sn})$ to changes in complexes **2** and **3**: A near-linear decrease in $\delta(^{119}\text{Sn})$ (Figure 4a) as the electron density on **2** is increased leads, for the more electron-rich **3**, to a reversal of the direction of change of $\delta(^{119}\text{Sn})$.

(2) The response of $\delta(^{103}\text{Rh})$ to changes in complex **3**: When ligand L has low nucleophilicity (benzonitrile), variations in electron-donating ability cause fairly large changes in $\delta(^{103}\text{Rh})$;

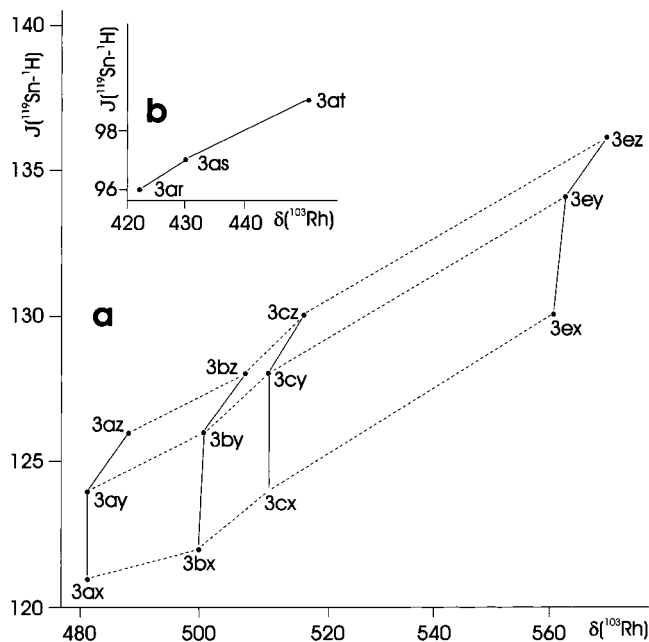


Figure 6. (a) Plot of $J(^{199}\text{Sn}-^1\text{H})$ vs $\delta(^{103}\text{Rh})$ for the complexes *trans*-[Rh(X)(H)(SnPh₃)(PPh₃)₂(L)] (**3**) with X and L varied: X = NCBPh₃ (a), N(CN)₂ (b), NCS (c), NCO (e); L = 4-MeO₂Cpy (x), py (y), 4-Me₂Npy (z). The complexes were prepared in situ; the solvent was dichloromethane. Data were recorded at -60 °C. Dotted line: X varied. Solid line: L varied. (b, Inset) Plot of $J(^{199}\text{Sn}-^1\text{H})$ vs $\delta(^{103}\text{Rh})$ for **3a**: L = 4-MeCOC₆H₄CN (r), C₆H₅CN (s), 4-Me₂NC₆H₄CN (t). The solvent was dichloromethane, and data were recorded at -60 °C.

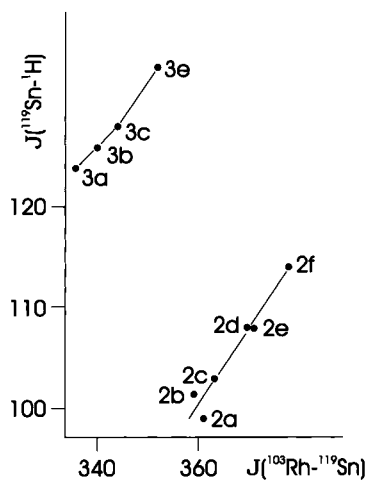


Figure 7. Plot of $J(^{199}\text{Sn}-^1\text{H})$ vs $J(^{103}\text{Rh}-^{119}\text{Sn})$ for the complexes [Rh(X)(H)(SnPh₃)(PPh₃)₂(L)] (**2**) and *trans*-[Rh(X)(H)(SnPh₃)(PPh₃)₂(L)] (**3**) with L = py and X varied: X = NCBPh₃ (a), N(CN)₂ (b), NCS (c), N₃ (d), NCO (e), O₂CCF₃ (f). The complexes were prepared in situ; the solvent was dichloromethane (toluene for f). Data for **2** were recorded at -25 °C; data for **3**, at -60 °C.

when L has higher nucleophilicity (pyridine), similar variations cause much smaller changes in $\delta(^{103}\text{Rh})$ (Figure 6).

(3) The response of $J(^{199}\text{Sn}-^1\text{H})$ to changes in complexes **2** and **3**: When py is replaced by 4-Me₂Npy in complex **2** the average increase in $J(^{199}\text{Sn}-^1\text{H})$ is ~ 7 Hz; when py is replaced by 4-Me₂Npy in complex **3**, the average increase in $J(^{199}\text{Sn}-^1\text{H})$ is only 2 Hz. The corresponding increases in $J(^{199}\text{Sn}-^1\text{H})$ on exchanging 4-MeO₂Cpy for py are 3–4 Hz for both **2** and **3**.

A three-center bond can be visualized as lying on a trajectory³⁰ leading from the individual starting compounds, here Ph₃SnH and a rhodium complex, to an oxidative addition product

in which the bond between tin and hydrogen no longer exists. The direction of movement along the trajectory defines a process as being one of oxidative addition or reductive elimination. In a finely balanced system, the three-center bond will be stable.

On moving along the trajectory, the tin atom, in a complex containing Rh, H, and Sn, will undergo a change in geometry from four-coordinate (in the full oxidative addition product) to five-coordinate as the interaction between Sn and H becomes stronger and, as the Rh–Sn and Rh–H bonds become weaker, will then return to four-coordinate geometry (free R₃SnH). The results described in (1), above, agree with this. The tin chemical shift is sensitive to Sn geometry, becoming more negative as the coordination number is changed from 4 to 5.²⁵ However, the facts that the reversal of the direction of change of $\delta(^{199}\text{Sn})$ is observed only in **3** with L = Me₂Npy and that this change occurs at values of $J(^{199}\text{Sn}-^1\text{H})$ that differ by as much as 10 Hz (Figure 4a) might suggest that the 4-Me₂Npy ligand itself, rather than the increased electron density that it conveys to the rhodium, is in some way responsible for the effect. Evidence against such an interpretation is found in the results for **2** (Figures 3 and 4a), which show no anomalies for complexes of 4-Me₂Npy. Studies involving a wider range of pyridines might help to clarify the situation.

The results described in (2) and (3), above, can be rationalized in terms of a transfer of electron density from rhodium to tin and hydrogen. As the electron density on rhodium is increased, a progressively larger fraction is transferred to Sn and H, which together act as an acceptor of electron density that is not readily taken up elsewhere. When the source of the increased electron density is the ligand positioned *trans* to tin (as in complex **3**), this transfer should be particularly efficient. If a buildup of electron density on rhodium is avoided in this way, the fact should be reflected in the rhodium chemical shift, which, as is observed, should then be relatively insensitive to such changes. With lower overall electron density on rhodium, any increase should become more evenly distributed and the influence on $\delta(^{103}\text{Rh})$ should be proportionately stronger (as observed).

Electron density transferred to tin can strengthen the Sn–H interaction and increase the contribution of $^1J(^{199}\text{Sn}-^1\text{H})$ to the observed coupling constant. $^1J(^{199}\text{Sn}-^1\text{H})$ has a negative sign and $^2J(^{199}\text{Sn}-^1\text{H})$ has a positive sign; thus any increase in the 1J component will subtract from changes in 2J , causing $^2J(^{199}\text{Sn}-^1\text{H})$ to appear smaller than might otherwise be expected. An effect matching this is observed for the most electron-rich complexes, **3**, with L = 4-Me₂Npy.

Interpretation of $J(^{199}\text{Sn}-^1\text{H})$. The value of $J(^{199}\text{Sn}-^1\text{H})$ correlates with the electron density on rhodium. With increasing $J(^{199}\text{Sn}-^1\text{H})$, ligands X appear in the order NCBPh₃, N(CN)₂, NCS, Cl, N₃, NCO, O₂CCF₃, ligands L in the order 4-MeO₂Cpy, py, 4-Me₂Npy, and phosphine ligands in the order P(4-C₆H₄F)₃, PPh₃, P(4-C₆H₄Me)₃, i.e., according to their electron donating abilities.

As **3** is made increasingly electron-rich, so it becomes more difficult to prepare (in situ), the yield diminishing until, with highly electron-donating combinations of ligands, no product **3** is formed. For **3**, the highest observed value of $J(^{199}\text{Sn}-^1\text{H})$ is 136 Hz (**3cz**); this appears to represent a limiting region beyond which the complexes (at -60 °C) are unstable.

Conclusion

The parameters that are most informative regarding potential influences on the three-center bond in complexes **2** and **3**,

(30) Crabtree, R. H.; Holt, E. M.; Lavin, M.; Morehouse, S. M. *Inorg. Chem.* **1985**, *24*, 1986.

$J(^{119}\text{Sn}-^1\text{H})$, $\delta(^{119}\text{Sn})$ and $\delta(^{103}\text{Rh})$, are insensitive to a variety of changes in ligands, suggesting that, within limits, these changes do not significantly alter either the electronic balance of the bond ($J(\text{Sn}-\text{H})$, $\delta(\text{Sn})$) or the electronic environment of rhodium ($\delta(\text{Rh})$). This can be seen for complexes **2** with X an N-donor ligand and L a pyridine, where the responses of $J(^{119}\text{Sn}-^1\text{H})$ and $\delta(^{119}\text{Sn})$ to variations in X and L are largely independent of whether X or L is varied. For complexes **3a–c.e.**, where the effects on $\delta(^{103}\text{Rh})$ of variations in L (pyridines) are minimal, the changes caused by varying L appear to be transmitted almost entirely to Sn and H. For the most electron-rich complexes (**3**), the data show trends consistent with events that are expected to occur close to the dissociation limit. The

reversal of the direction of change of $\delta(^{119}\text{Sn})$ for complexes having the most nucleophilic pyridine is a predictable consequence of a transition from five- to four-coordination for tin. For **3**, the diminishing responses of $^2J(^{119}\text{Sn}-^1\text{H})$ to variations in L are likely to reflect increased contributions from $^1J(^{119}\text{Sn}-^1\text{H})$ as the Sn–H bond becomes stronger.

Acknowledgment. Thanks are expressed to the University of the Witwatersrand and the NRF for financial support and to Professor J. Jeener and Professor M. H. Levitt as well as an anonymous reviewer for advice concerning signs of NMR data.

IC991054G